Australian Journal of Earth Sciences

An International Geoscience Journal of the Geological Society of Australia

ISSN: 0812-0099 (Print) 1440-0952 (Online) Journal homepage: http://www.tandfonline.com/loi/taje20

Late Paleozoic geology of the Queensland Plateau (offshore northeastern Australia)

U. Shaanan, G. Rosenbaum, D. Hoy & N. Mortimer

To cite this article: U. Shaanan, G. Rosenbaum, D. Hoy & N. Mortimer (2018): Late Paleozoic geology of the Queensland Plateau (offshore northeastern Australia), Australian Journal of Earth Sciences, DOI: 10.1080/08120099.2018.1426041

To link to this article: https://doi.org/10.1080/08120099.2018.1426041

Published online: 11 Feb 2018.

AUSTRALIAN JOURNAL OF EARTH SCIENCES, 2018
https://doi.org/10.1080/08120099.2018.1426041

Late Paleozoic geology of the Queensland Plateau (offshore northeastern Australia)

U. Shaanan [a], G. Rosenbaum [a], D. Hoy [a] and N. Mortimer [b]

[a]School of Earth and Environmental Sciences, The University of Queensland, Brisbane, Australia; [b]GNS Science, Private Bag 1930, Dunedin 9054, New Zealand

ABSTRACT

The southwestern Pacific region consists of segmented and translated continental fragments of the Gondwanan margin. Tectonic reconstructions of this region are challenged by the fact that many fragmented continental blocks are submerged and/or concealed under younger sedimentary cover. The Queensland Plateau (offshore northeastern Australia) is one such submerged continental block. We present detrital zircon geochronological and morphological data, complemented by petrographic observations, from samples obtained from the only two drill cores that penetrated the Paleozoic metasedimentary strata of the Queensland Plateau (Ocean Drilling Program leg 133, sites 824 and 825). Results provide maximum age constraints of 319.4 ± 3.5 and 298.9 ± 2.5 Ma for the time of deposition, which in conjunction with evidence for deformation, indicate that the metasedimentary successions are most likely upper Carboniferous to lower Permian. A comparison of our results with a larger dataset of detrital zircon ages from the Tasmanides suggests that the Paleozoic successions of the Queensland Plateau formed in a backarc basin that was part of the northern continuation of the New England Orogen and/or the East Australian Rift System. However, unlike most of the New England Orogen, a distinctive component of the detrital zircon age spectra of the Mossman Orogen is also recognised, suggesting the existence of a late Paleozoic drainage system that crossed the northern Tasmanides *en route* from the North Australian Craton. A distinctive shift from abraded zircon grains to grains with well-preserved morphology at *ca* 305 Ma reflects a direct drainage of first-cycle sediments, most likely from an outboard arc and/or backarc magmatism.

ARTICLE HISTORY
Received 31 July 2017
Accepted 5 January 2018

KEYWORDS
Queensland Plateau; ODP; terrane analysis; paleodrainage; zircon; New England Orogen; Mossman Orogen; Gondwana; Australia; Zealandia

Introduction

Eastern Australia (Tasmanides) and the continental southwestern Pacific region (Zealandia) consist of a collage of continental fragments and sedimentary basins that formed along the margin of southeastern Gondwana during the Phanerozoic (Figure 1a; Glen, 2005; Mortimer *et al.*, 2017; Rosenbaum, 2018). Rocks in these regions record a prolonged subduction history of intermitted extensional and contractional episodes that were likely driven by the mobility of the subduction boundary (Collins, 2002).

Much of the Paleozoic and Mesozoic metasedimentary successions of eastern Australia and Zealandia (hereinafter basement rocks) are either submerged or concealed under younger sedimentary cover. Basement rocks of these regions typically contain a large component of multi-cycled Gondwanan detritus (Fergusson & Henderson, 2015; Fergusson, Henderson, & Offler, 2017; Foster & Goscombe, 2013; Glen, 2013; Glen, Belousova, & Griffin, 2016). Detrital zircon studies in eastern Australia and the southwestern Pacific region have shown that both sedimentary (Shaanan & Rosenbaum, 2018; Sircombe, 1999) and magmatic (Buys, Spandler, Holm, & Richards, 2014; Tapster, Roberts, Petterson, Saunders, & Naden, 2014) recycling took place. Shaanan, Rosenbaum, and Sihombing (2017) have recently demonstrated that the occurrence and absence of specific age populations, and the age distribution of the recycled/inherited Paleoproterozoic and Archean ages in geochronological datasets of detrital zircon, provide a detrital-fingerprint that can illuminate sediment pathways and recycling of detritus between the different domains of the Tasmanides.

The Queensland Plateau is a submerged continental block offshore northeastern Australia (Figure 1a, b). The metasedimentary strata of this plateau are thought to be part of the Gondwanan continental margin (Ewing, Hawkins, & Ludwig, 1970; Feary, Champion, Bultitude, & Davies, 1993; Henderson, Davis, & Fanning, 1998; Mortimer, Hauff, & Calvert, 2008). However, while some authors suggested that the Queensland Plateau correlates with rocks of the Mossman Orogen (Feary *et al.*, 1993), others suggested it to be the along-strike continuation of the New England Orogen (Henderson *et al.*, 1998; Mortimer *et al.*, 2008). In this study, we analysed detrital zircon grains from samples from the only two drill sites that reached the metasedimentary basement rocks of the Queensland Plateau (Ocean Drilling Program [ODP], leg 133, sites 824 and 825; previously studied for petrography and whole-rock chemistry by Mortimer *et al.*, 2008). In addition, we conducted a quantitative morphological classification of dated grains,

CONTACT U. Shaanan u.shaanan@uq.edu.au

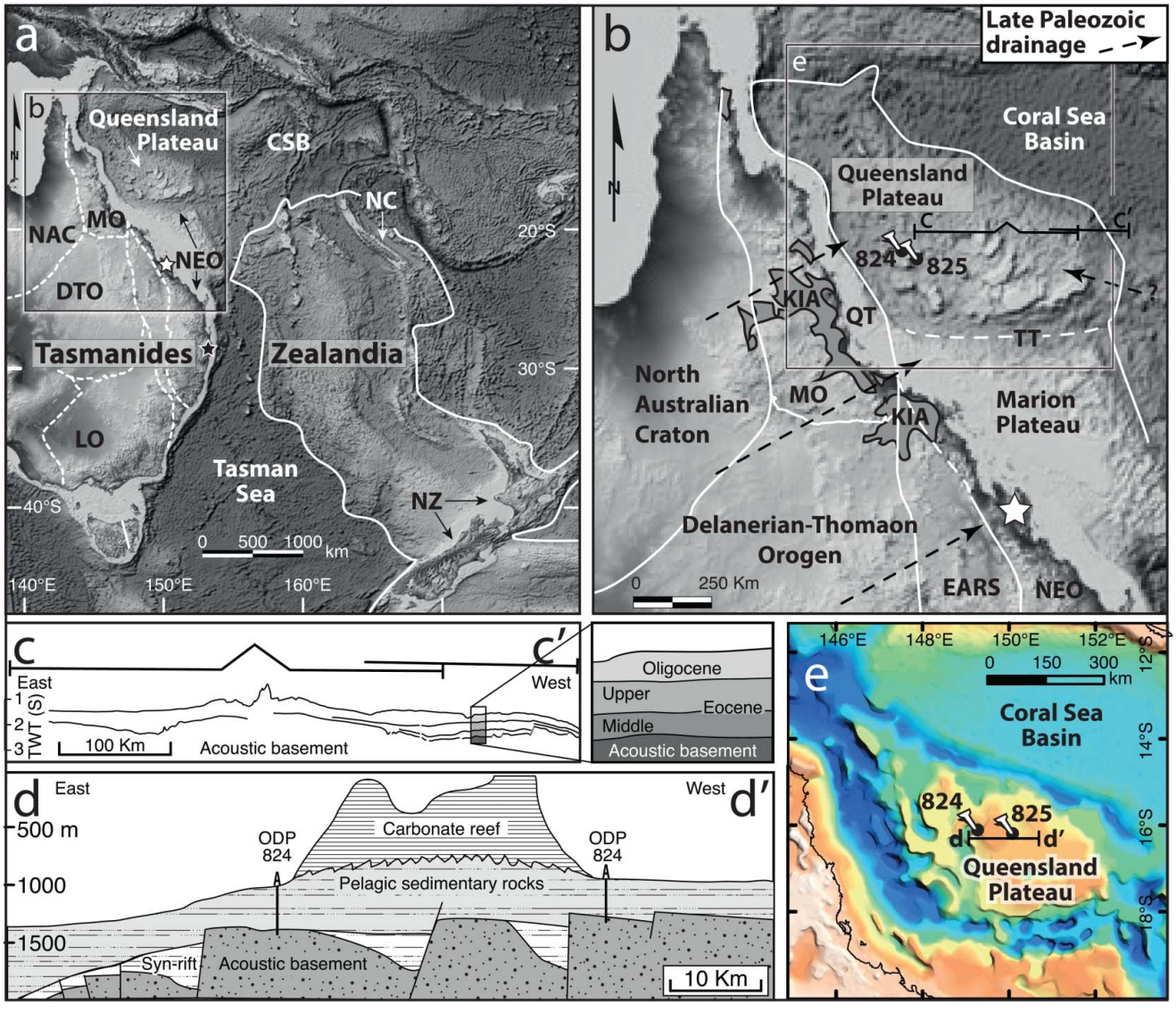

Figure 1. Maps and cross-sections of the study area. (a, b) Relief model of land topography and ocean bathymetry of eastern Australia and the southwestern Pacific region. Panel b shows the position of ODP drill sites 824 and 825 (Leg 133) and the proposed connection with the New England Orogen and east Australian Rift System. (c) Interpretation of two east–west seismic transects (C–C' on panel b) and corresponding chronostratigraphy across the Queensland Plateau (after Mutter, 1977). (d) Schematic east–west cross-section (D–D' on panel e) of ODP sites 824 and 825, based on site-survey seismic tracks in the vicinity of the sites (after Feary *et al.*, 1993). (e) Basement topography of the Queensland Plateau based on the OZ Seebase study (Frogtech, 2005), whereby cold colours are basement depressions and warm colours are basement highs. White and black stars (in a and b) denote localities of the Shoalwater Formation and Neranleigh–Fernvale beds, respectively. Abbreviations: CSB, Coral Sea Basin; DTO, Delamerian-Thomson Orogen; EARS, East Australian rift System; KIA, Kennedy Igneous Association (simplified); LO, Lachlan Orogen; MO, Mosman Orogen; NAC, North Australian Craton; NC, New Caledonia; NEO, New England Orogen; NZ, New Zealand; QT, Queensland Trough; TT, Townsville Trough; TWT (S), two-way-travel time in seconds.

and a petrographic investigation. By comparing our results with data from the Paleozoic strata of proximal domains in the Tasmanides, we provide new constraints on the age, stratigraphic correlation, paleodrainage and tectonic record of this part of the Gondwanan margin.

Geological setting

The Queensland Plateau is situated in the Coral Sea, and is bounded by deep marine troughs to the west (Queensland Trough) and south (Townsville Trough) from Silurian–Devonian rocks of the Mossman Orogen, and Devonian–Triassic rocks of the New England Orogen (Figure 1a, b). Rocks of the Mossman and New England orogens record several phases of deformation, including deformation associated with the so-called Hunter–Bowen Orogeny that took place from the middle Permian to the Late Triassic (Holcombe *et al.*, 1997; Hoy & Rosenbaum, 2017; and references therein). Rocks in the Queensland Plateau include a deformed metasedimentary succession, intruded by intermediate igneous rocks (Feary *et al.*, 1993), and covered by Cenozoic (predominantly Eocene to Miocene) carbonate platform strata (Figure 1c, d; Betzler & Chaproniere, 1993; Betzler, Kroon, Gartner, & Wei, 1993; Brachert, Betzler, Davies, & Feary, 1993). A continental crustal nature of the Queensland Plateau has been suggested based on seismic (Ewing *et al.*, 1970), petrographic (Feary

et al., 1993) and geochemical (Mortimer *et al.*, 2008) data. Seismic data show that the present-day bathymetry of the Queensland Plateau corresponds with the topography of the acoustic basement (Figure 1c, d; Mutter, 1977). Gravity lineaments attributed to structures within the basement of the Queensland Plateau are parallel to the structural grain of Paleozoic rocks onshore Australia (Falvey & Taylor, 1974; Mutter, 1977).

Igneous and metasedimentary rocks were recovered from ODP drill sites 824 and 825, which are located 43 km from each other (Figure 1b–e). Holes 824C and 824D penetrated approximately 25 m into the basement with 5% recovery, and hole 825 penetrated approximately 13 m with 13% recovery (Feary *et al.*, 1993). Petrographic descriptions of the basement rocks, as well as technical information on drilling and seismic interpretation are reported by Feary *et al.* (1993) and are summarised below.

The basement rocks in both drill sites consist of metamorphosed siltstone and sandstone with a composition of subquartzose litharenites (Feary *et al.*, 1993; Mortimer *et al.*, 2008). The absence of metamorphic biotite or garnet suggests sub- to lower-greenschist facies metamorphism. The metasedimentary succession is intruded (in ODP 824) by granodiorite and tonalite (Feary *et al.*, 1993). The metasedimentary rocks are predominantly characterised by bedding-parallel fabric that, in places, is overprinted by one or two crenulation fabrics (Feary *et al.*, 1993). A metasedimentary sample of argillite from ODP 825 yielded whole-rock K–Ar weighted mean age of 240 $\pm$ 4 Ma (2σ); however, it is unclear whether this age represents the age of detrital grains, metamorphism, cooling or any combination of mixed ages (Mortimer *et al.*, 2008).

Methodology

Thin-sections used for this study were made at GNS Science and at the University of Queensland. Drill core samples (Appendix 1) were fragmented to monomineralic grains using high-voltage pulsed power discharges (SelFrag Lab^{TM}) at Macquarie University. Use of high-voltage pulsed power discharges for grain liberation significantly diminishes the risk of producing zircon fragments by crushing individual grains. This mineral-liberation method thus provides higher confidence in the inclusion of all grains in their original morphology and proportion of age populations.

Mineral separation was conducted at The University of Queensland. Magnetic minerals were removed using a Frantz Magnetic Separator and the non-magnetic fraction was put in di-iodomethane heavy liquid to obtain heavy mineral concentrates. All zircon grains larger than approximately 30 μm were handpicked using a binocular microscope and mounted in non-reactive epoxy resin. The mounted grains were polished to expose their inner sections and growth zonation, and imaged with an electron microscope.

Detrital zircon geochronology was conducted using a Laser Ablation Inductively Coupled Plasma Mass Spectrometer (LA-ICP-MS) at the Queensland University of Technology. Data reduction was conducted using Iolite v3.5 (Paton, Hellstrom, Paul, Woodhead, & Hergt, 2011) and VizualAge v2016.06 (Petrus & Kamber, 2012). Age calculations and data visualisation were produced using DensityPlotter (Vermeesch, 2012) and Isoplot v4.15 (Ludwig, 2003).

The interpretation presented herein considers the most robust data with discordance of $<$10% and after exclusion of analyses that yielded anomalously high trace element compositions (following the procedure described in Appendix 2). Data are reported in the supplemental material, and specific information regarding the analytical procedures is detailed in Appendix 2. Isotopic composition of one analysis yielded an apparently concordant date of 99.69 $\pm$ 2.5 Ma (sample QP-825), which is inconsistent with the geological context and may reflect a contamination of the drill-core samples (possibly from overlying strata, during drilling), or an unnoticed igneous vein within the sedimentary rock. Isotopic data from this analysis are included in the supplemental material; however, given that the data do not appear to be geologically meaningful, we do not include the results of this analysis in the interpretation and discussion.

The roundness of all near-concordant zircon grains was quantified following the method of Shaanan and Rosenbaum (2018). Roundness was determined using a scale of 1–5 that represents anhedral to euhedral morphology, respectively (Figure 2). This value was averaged for each age population and normalised to percent such that roundness of 100% indicates a highly abraded population, while a low roundness percentage indicates a population consisting of well-preserved grains. Age populations were determined by combined consideration of kernel density estimates (Sircombe & Hazelton, 2004) and relative probability plots. The standard deviation of the roundness value for a calculated age population reflects the variation of roundness values relative to the mean roundness percentage. Large standard deviation, therefore, reflects large variations in abrasion, and may indicate that an age population consists of grains that underwent different transportation histories, and were possibly derived from different sources (i.e. mixed provenance within a single age population).

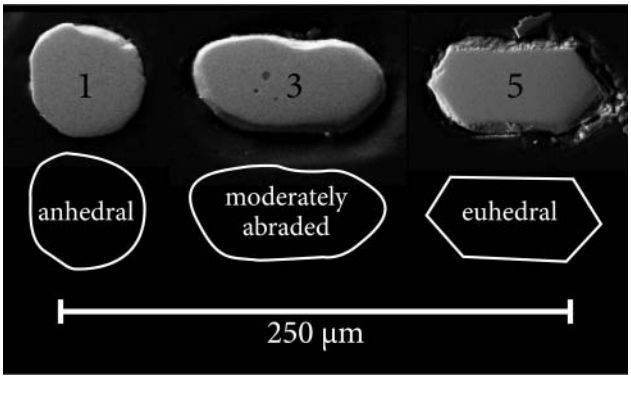

Figure 2. Representative detrital zircon grains from this study showing a roundness scale whereby 1 represents anhedral grains for which the external crystallographic form is not evident and 5 represents well-preserved crystal habit of well-preserved rims (following Shaanan & Rosenbaum, 2018).

Results

Microstructure

Samples from ODP drill cores 824 and 825 (Appendix 1) collectively contain the following lithologies: (1) foliated metasandstone and metasiltstone, (2) tectonised hypabyssal andesite, and (3) quartz and calcite veins that cross-cut the two host lithologies (Figure 3a). At least three generations of penetrative fabrics are recognised, showing different intensity, orientation and cross-cutting relationships. A prominent fabric defined by quartz–mica domains (S_1) is cross-cut by pressure solution seams (S_2; Figure 3b, e). A conjugate set of incipient crenulation cleavage (S_{3a}, S_{3b}) overprints S_1 and S_2 (Figure 3c). Both S_1 and S_2 fabrics are clearly evident across the contact of the metasedimentary rock and the magmatic intrusion (Figure 3d). Furthermore, the occurrence of S_1 fabric in quartz veins that cross the contact between the intrusion and the metasedimentary rock indicates that deformation postdated the intrusion.

Geochronology

U–Th–Pb isotopic compositions of detrital zircon grains from the metasedimentary core samples yielded a total of 195 meaningful concordant ages (63 ages from site 824 and 132 ages from site 825). In order to address internal variations in the proportions of age populations, and to obtain sufficient yield of zircon ages to permit a meaningful discussion on the age populations of the succession, the different metasedimentary samples of each core were merged (see Appendix 1 for specific core sections). Merging samples of successive beds within a coherent succession was previously shown to minimise the effect of natural variation that occurs in the proportion of ages, thus leading to a more accurate characterisation of the overall age spectra of the succession (Shaanan *et al.*, 2017). Despite repeated attempts to extract zircon grains and date the hypabyssal andesite, no concordant analyses were obtained. Therefore, the time of emplacement can only be constrained as postdating deposition of the host rock, and predating deformation features that overprint it. Geochronological results are presented in Figures 4 and 5, and in the supplemental material.

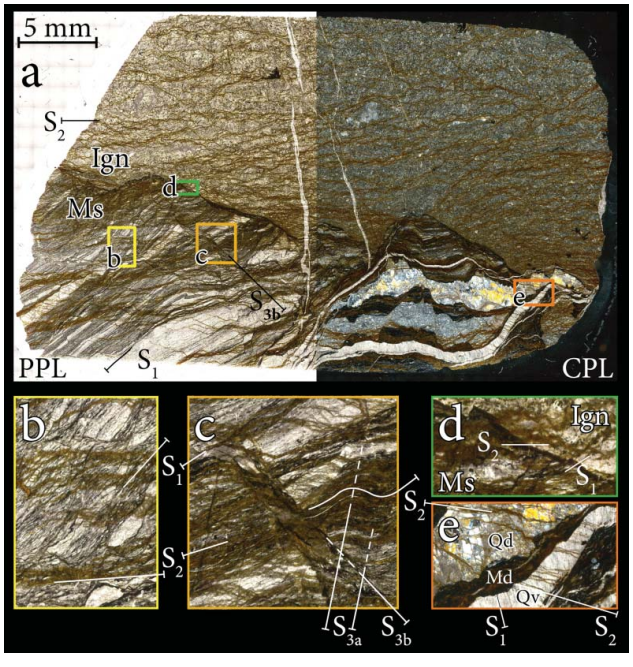

Figure 3. Composite photomicrograph of a representative sample from the Queensland Plateau, which is intruded by an andesite dyke. The sample is from ODP drill site 824D (Appendix 1). The right side is taken under cross-polarised light, and the left side is under plane-polarised light. Abbreviations: Ign, igneous rock; Md, mica domain; Ms, metasedimentary rock; Qd, quartz domain; Qv, quartz vein.

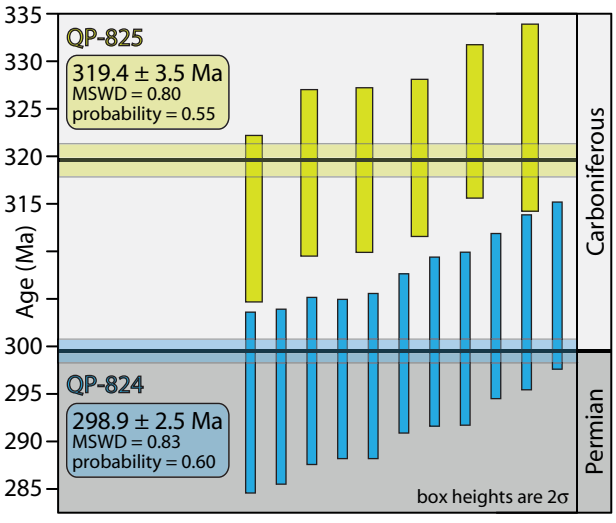

Figure 4. Youngest clusters of overlapping concordant ages for samples 825 (yellow, $n = 6$) and 824 (blue, $n = 11$) providing robust late Carboniferous and early Permian maximum age constraint for the time of deposition.

Maximum age constraint for the time of deposition

The youngest geologically meaningful near-concordant ages from samples QP-825 and QP-824 are 302.3 ± 8.3 Ma and 293.1 ± 8.9 Ma, respectively. These ages overlap within two-sigma error with each other and with the sequences of older ages from both samples. The youngest clusters of overlapping concordant ages provide robust late Carboniferous (Pennsylvanian, 319.4 ± 3.5 Ma, $n = 6$) and early Permian (298.9 ± 2.5 Ma, $n = 11$) maximum age constraints for the time of deposition (Figure 4).

Detrital zircon age spectra

Examination of the distribution of ages in cumulative proportion curves and in kernel density estimates show that the spectra of the rocks from the two drill holes have somewhat similar age populations, but in slightly different proportions (Figure 5a, c). While the spectra of sample QP-825 consist of age populations of 2650, 1546, 1066, 577 and 376 Ma, sample QP-824 consists of age populations of 1608, 500 and 314 Ma (Figure 5c). Both samples QP-825 and QP-824 contain a relatively large fraction of dates that are older than Neoproterozoic (over 50% and over 30%, respectively; Figure 5a).

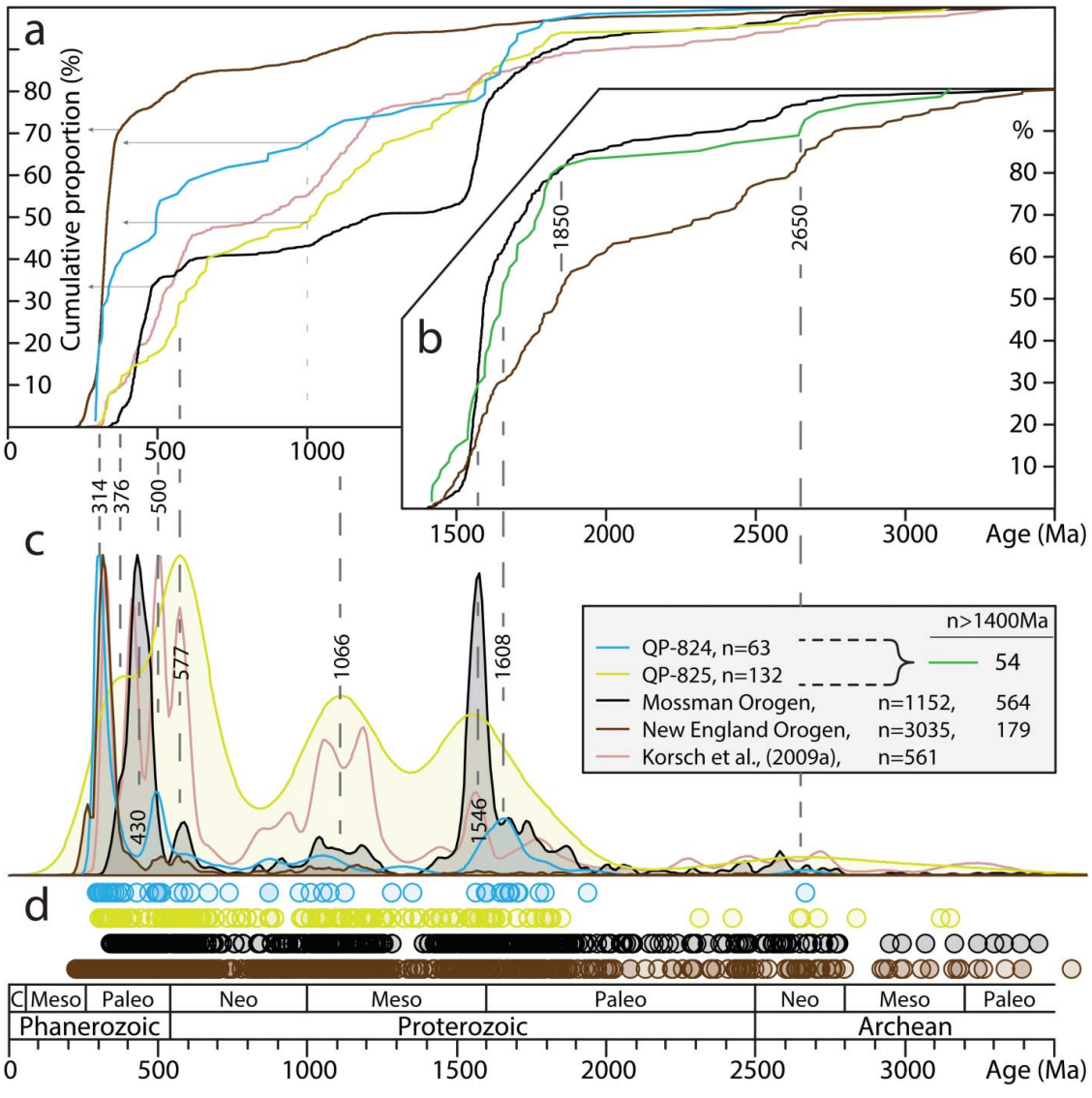

Figure 5. Detrital zircon age spectra and youngest ages of basement samples of drill cores from sites 824 and 825 (ODP leg 133, for location see Figure 1b, e). Data from this study are plotted over detrital zircon data from the Mossman (n = 1152) and New England (n = 3035) orogens (after Shaanan *et al.*, 2017, and references therein), and over lower Carboniferous quartz-rich sandstone data of the Shoalwater Formation and Neranleigh–Fernvale beds (n = 561, after Korsch *et al.*, 2009a; see locations in Figure 1). (a) Cumulative proportion curves. (b) Cumulative proportion of the age range that predate 1400 Ma. (c) Kernel Density Estimates. (d) Age distribution (circles). The timeline at the base of the figure corresponds to all figure panels and is abbreviated conventionally.

Morphological classification

Morphological classification was conducted on the corresponding grains of all 195 meaningful, near-concordant ages. The youngest age populations of both samples are the least rounded (54% and 61%), while older age groups consist of corresponding higher roundness values (Figure 6a, b). Examination of the combined data of the youngest age populations from the two samples (i.e. ages that are <420 Ma, n = 45; Figure 6c), show that the youngest cluster of these ages (<305 Ma, n = 13) consists of a significantly less abraded grain assemblage, with average roundness value of 25% (Figure 6c). In contrast, grains with ages between 420 and 305 Ma exhibit roundness values that are equivalent to that of the older age groups (Figure 6).

Discussion

Implications for the tectonic history of the Queensland Plateau

The igneous intrusion found in sample QP-824 and the development of multiple foliation fabrics must be younger than the early Permian constraint for the age of deposition of the metasedimentary rocks (Figures 3 and 4). This age constraint suggests that the whole-rock K–Ar age of 240 ± 4 Ma (Mortimer *et al.*, 2008) is either a metamorphic or a cooling age (or possibly a mixed age). The occurrence of multiple overprinting foliation fabrics that are Permian or younger, in conjunction with a 240 Ma metamorphism/cooling age (Mortimer *et al.*, 2008), suggests that metamorphism and deformation took place during the middle Permian to Late Triassic

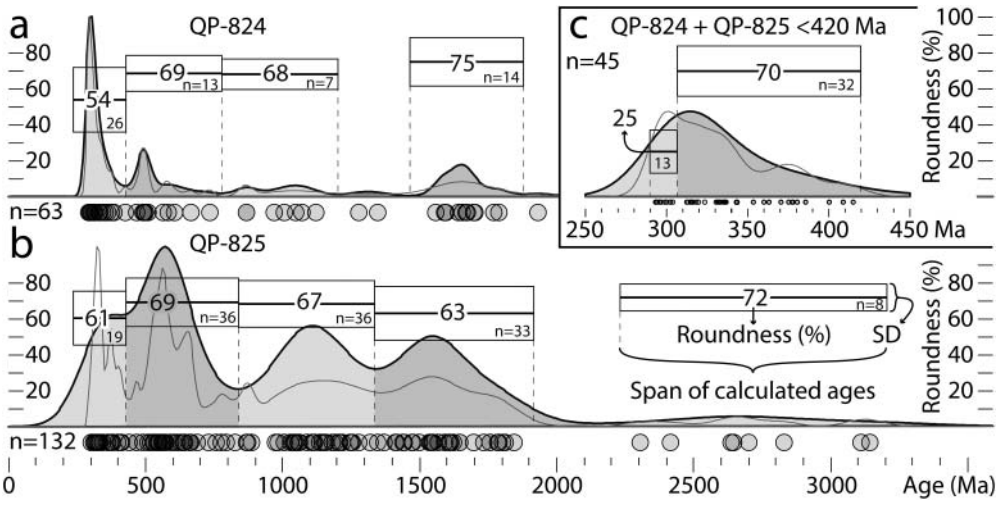

Figure 6. Quantitative classification of roundness (abrasion) of detrital zircon from the Queensland Plateau. Rectangles reflect values of calculated roundness whereby the vertical axis corresponds to the standard deviation (SD) of the calculated average (in percent) and the horizontal axis reflects the bracketed time span, as determined by the combination of kernel density estimate (black stroke) and relative probability (grey stroke). (a) Sample QP-824. (b) Sample QP-825. (c) Ages that are younger than 420 Ma from samples QP-824 and QP-825 combined.

(270–230 Ma) Hunter–Bowen Orogeny (e.g. Holcombe *et al.*, 1997; Hoy & Rosenbaum, 2017; and references therein). Deformation that is associated with this orogenic event is evident in the Mossman Orogen (e.g. Davis & Henderson, 1999) and throughout the New England Orogen (Hoy & Rosenbaum, 2017; and references therein). Emplacement of the igneous intrusion occurred prior to the generation of the first structural fabric, thus either before or during Hunter–Bowen deformation.

Detrital zircon age spectra

Examination of the age spectra from samples QP-825 and QP-824 against detrital zircon data compilation of Permian and older sedimentary rocks of the Mossman (n = 1152) and New England (n = 3035) orogens (Shaanan *et al.*, 2017) shows that the youngest age populations correspond to those of the New England Orogen (Figure 5c). In contrast, the older components of the samples from the Queensland Plateau better correspond to the age spectra of the Mossman Orogen (Figure 5c). Specifically, a prominent age population at *ca* 314 Ma in OP-824 (Figure 5a, c) corresponds to the major youngest age population of the New England Orogen, whereas age populations at approximately 1608 Ma, 1546 Ma, 1066 Ma and 577 Ma better match the age spectra of the Mossman Orogen. Separate examination of the >1400 Ma cumulative proportions of the merged data from the Queensland Plateau (n = 54) against that of the Mossman (n = 565) and New England (n = 179) orogens, reveals approximately similar proportions of ages to those obtained for the Mossman Orogen, with occurrences of age populations that are characteristic to the New England Orogen (e.g. of 2650 Ma, 1850 Ma and 1540–1400 Ma; Figure 5b).

The general correspondence of age populations of the Queensland Plateau data to age populations from both the New England and Mossman datasets, suggests that the Queensland Plateau samples consist of detritus that was derived from both orogens and/or their respective sources. In terms of a basic orogen-scale correlation, the better fit of the younger ages with the New England dataset, and older ages with the Mossman dataset likely resulted from the different proportion of ages in the two datasets. The age spectra of the New England Orogen predominantly consist of detritus that underwent a relatively short time span from source to sink (over 70% of ages are within the youngest age population), whereas the age spectra of the Mossman Orogen are dominated by prolonged recycled and/or inherited detritus (less than 35% of ages are within the youngest age population). In other words, the New England and Mossman orogens are the least and most recycled components of the Tasmanides, respectively (Shaanan *et al.*, 2017), and their mixture therefore impacts different time spans of the age spectra differently. Such a distribution of ages serves to explain the high resemblance of old ages between the data from the Queensland Plateau to the Mossman dataset (Figure 5b) despite the occurrence of a New England signature in the younger populations (Figure 5a, c). Furthermore, variations in the mixture ratio of detritus from these two components serve to explain the differences between the two samples. Interestingly, however, the major age component of the Mossman Orogen (*ca* 430 Ma), which occurs throughout the dataset of the orogen (Shaanan *et al.*, 2017), is absent from both Queensland Plateau samples.

Tectonic association of the Queensland Plateau

The fact that the youngest ages (Figure 4) and youngest age populations in the Queensland Plateau correspond to that of the New England Orogen (Figure 5c), and that the youngest prominent age population of the Mossman Orogen is absent

from the data of the Queensland Plateau, suggests that the basement rocks of the Queensland Plateau constitute a part of the New England Orogen. This is consistent with previous suggestions that the Queensland Plateau is the submerged along-strike continuation of the New England Orogen (Henderson *et al.*, 1998; Mortimer *et al.*, 2008), which possibly extends farther north into Permian–Triassic igneous rocks in Papua New Guinea (Pigram & Panggabean, 1984). Furthermore, age spectra from lower Carboniferous quartz-rich sandstones in the New England Orogen (Shoalwater Formation and Neranleigh–Fernvale beds; Figure 1a, Korsch *et al.*, 2009a) include age populations that resemble those found in the Queensland Plateau (Figure 5a, c). These data were, in part, affected by a non-random selection bias, as the authors reported targeting zircon grains with specific morphologies (Korsch *et al.*, 2009a), meaning that the proportion of ages was distorted. Nonetheless, the occurrence of age populations that resemble those from the Queensland Plateau samples further supports the suggested association with the New England Orogen or its original provenance. The Shoalwater/Neranleigh–Fernvale rocks were highlighted by Korsch *et al.* (2009a) as anomalously mature in composition and interpreted as reflecting derivation of detritus from the continental interior.

Late Carboniferous and early Permian constraints on the time of deposition, in conjunction with mixed composition of age spectra of the New England Orogen and the continental interior (that approximates the Mossman signature), suggest that the basement of the Queensland Plateau may also be the northern continuation of a continental-scale rift system that developed in the early Permian west of the New England Orogen (the early Permian East Australian Rift System; Figure 1a, b; i.e. Korsch, Totterdell, Cathro, & Nicoll, 2009b). This suggestion is consistent with the occurrence of detritus of mixed maturity (subquartzose litharenites; Feary *et al.*, 1993; Mortimer *et al.*, 2008), which is typical for backarc basins (e.g. Cawood, Hawkesworth, & Dhuime, 2012). Early Permian backarc basins occur west (Korsch *et al.*, 2009b) and within the New England Orogen (e.g. Leitch, 1988; Shaanan, Rosenbaum, & Wormald, 2015). It is therefore reasonable that the samples obtained from the basement of the Queensland Plateau embody a northern expression of an early Permian continental extensional backarc system.

The age spectra of the youngest age populations found in the samples from the Queensland Plateau consists of abundant late Carboniferous ages (*ca* 314 Ma; Figure 5c), with minor occurrence of earliest Permian ages (Figure 4). Similar proportions of youngest age populations from early Permian (backarc) basins within the New England Orogen have been suggested to reflect mixed drainage of recycled sediments from a Carboniferous forearc region and an oceanward positioned early Permian arc (Campbell, Rosenbaum, Shaanan, Fielding, & Allen, 2015; Shaanan & Rosenbaum, 2018; Shaanan *et al.*, 2015). The relatively high deviation in the morphology of youngest age populations (mostly evident in sample QP-824; Figure 6a) implies that these age populations consist of polymodal detritus that underwent different transportation histories. The abrupt shift from pre-305 Ma highly abraded (i.e. recycled and/or from distal sources) zircon grains to post-305 Ma well-preserved (first-cycle) grains marks the onset of a proximal juvenile magmatic source, and suggests that the age of the younger, first-cycle grains closely approximate the age of deposition. One possible source for these first-cycle sediments may be the Carboniferous and early Permian Kennedy Igneous Association, which represents widespread magmatism in northeastern Queensland (Figure 1b). The geodynamic context of the Kennedy Igneous Association is not fully understood, but has been suggested to be associated with regional extension (Jell, 2013). The position of the postulated backarc succession of the Queensland Plateau east of the Kennedy Igneous Association, implies that the latter represents widespread backarc magmatism. Whether this first-cycle youngest population derived from backarc magmatism and/or an oceanward position magmatic arc is unclear; however, its occurrence is consistent with the suggestion that during the early Permian, the New England Orogen was positioned in a hot extensional backarc setting (Cawood, Leitch, Merle, & Nemchin, 2011; Korsch *et al.*, 2009b; Little *et al.*, 1992; Rosenbaum, Li, & Rubatto, 2012; Shaanan *et al.*, 2015).

Implications for a late Paleozoic drainage system

Our results revealed a prominent 1600–1500 Ma age population of sedimentary detritus in the Queensland Plateau (Figure 5a–c). Within Paleozoic metasedimentary rocks of the Tasmanides, these ages occur as prominent populations almost solely in the Mossman Orogen (Shaanan *et al.*, 2017), and its recognition elsewhere has been suggested to represent a derivation from the continental interior (i.e. Korsch *et al.*, 2009a). The appearance of this age population in the age spectra of the northern continuation of the New England Orogen (i.e. in the Queensland Plateau) demonstrates a recycling hierarchy whereby detritus that is characteristic to the Mossman Orogen were delivered to the northernmost New England Orogen. The absence of the prominent *ca* 430 Ma youngest age population of the Mossman Orogen in the Queensland Plateau age spectra (Figure 5c) indicates an incomplete occurrence of Mossman age spectra. The fact that the age population of *ca* 430 Ma occurs throughout the dataset of the Mossman Orogen (Shaanan *et al.*, 2017), suggests derivation from drainage of the primary provenance of the Mossman strata (i.e. North Australia Craton; Figure 1a, b). It appears, therefore, that the late Paleozoic drainage system of the northern Tasmanides transported detritus of the same (original) sources to that of the Mossman Orogen, into an ever-growing and oceanward progressing continental margins of the Australian plate (Figure 1a).

Conclusions

Detrital zircon data from two drill sites from the Queensland Plateau comprise 195 near-concordant U–Th–Pb ages coupled with quantitative grain morphology. The data indicate late Carboniferous (319.4 ± 3.5) and early Permian (298.9 ±

2.5 Ma) maximum ages of deposition. The following three patterns were recognised in the detrital zircon age populations from the Queensland Plateau samples: (1) similar age spectra and correspondence of the youngest ages to that found in eastern Australian early Permian backarc basins. This suggests that Devonian–Carboniferous subduction-related rocks of the New England Orogen constitute a major source. (2) Significantly lower abrasion of grains that are younger than 305 Ma, suggesting a direct (first-cycle) derivation of the youngest component from contemporaneous subduction-related magmatism. (3) The occurrences of age population that is, within the Tasmanides, characteristic of the Mossman Orogen, in conjunction with the absence of the youngest and most prominent population of the Mossman Orogen (*ca* 430 Ma) suggest that the Queensland Plateau received detritus that was sourced from a similar drainage system to that which provided detritus to the Mossman Orogen, possibly from the North Australian Craton.

The combination of continental and first-cycle detritus suggests an early Permian continental backarc setting for the Queensland Plateau. The occurrence of multiple overprinting foliation fabrics, coupled with a Middle Triassic metamorphic/cooling age in the lower Permian rocks, suggests that the metasedimentary succession of the Queensland Plateau underwent deformation in the course of middle Permian to Late Triassic Hunter–Bowen Orogeny. The evidence for Hunter–Bowen deformation in the Queensland Plateau constitutes the northeastern-most known extent of this last major orogenic event in the Tasmanides.

Acknowledgements

This study was funded by International Ocean Drilling Program ANZIC Special Analytical Funding (2016, Shaanan, Rosenbaum and Mortimer). We thank the IODP stuff of Kochi Core Center (Japan) for providing us access to ODP core samples (sample request 46765IODP). The manuscript benefitted from comments by Carl Spandler, Bob Henderson and Rashed Abdullah.

Disclosure statement

No potential conflict of interest was reported by the authors.

Funding

This study was funded by International Ocean Drilling Program ANZIC Special Analytical Funding (2016, Shaanan, Rosenbaum and Mortimer).

Supplementary papers

Table: U–Pb isotope and trace-element data.

ORCID

U. Shaanan http://orcid.org/0000-0003-1674-6184
G. Rosenbaum http://orcid.org/0000-0002-2544-093X
D. Hoy http://orcid.org/0000-0002-3052-6383
N. Mortimer http://orcid.org/0000-0002-6812-3379

References

Belousova, E. A., Griffin, W. L., O'Reilly, S. Y., & Fisher, N. I. (2002). Igneous zircon: Trace element composition as an indicator of source rock type. *Contributions to Mineralogy and Petrology, 143*(5), 602–622.

Betzler, C., & Chaproniere, G. C. H. (1993). Paleogene and Neogene larger foraminifers from the Queensland Plateau; biostratigraphy and environmental significance. In J. A. McKenzie, P. J. Davies, A. Palmer-Julson, et al. (Eds.), *Proceedings of the Ocean Drilling Program, Scientific Results,* Vol. **133** (pp. 51–66). College Station, TX: Ocean Drilling Program, doi:10.2973/odp.proc.sr.133.210.1993.

Betzler, C. G., Kroon, D., Gartner, S., & Wei, W. (1993). Eocene to Miocene chronostratigraphy of the Queensland Plateau; control of climate and sea level on platform evolution. In J. A. McKenzie, P. J. Davies, A. Palmer-Julson, et al. (Eds.), *Proceedings of the Ocean Drilling Program, Scientific Results,* Vol. **133**, (pp. 281–289). College Station, TX: Ocean Drilling Program, doi:10.2973/odp.proc.sr.133.211.1993.

Black, L. P., Kamo, S. L., Allen, C. M., Davis, D. W., Aleinikoff, J. N., Valley, J. W., … Foudoulis, C. (2004). Improved $^{206}Pb/^{238}U$ microprobe geochronology by the monitoring of a trace-element-related matrix effect; SHRIMP, ID–TIMS, ELA–ICP–MS and oxygen isotope documentation for a series of zircon standards. *Chemical Geology, 205*(1–2), 115–140.

Brachert, T. C., Betzler, C. G., Davies, P. J., & Feary, D. A. (1993). Climatic change; control of carbonate platform development (Eocene–Miocene, Leg 133, northeastern Australia). In J. A. McKenzie, P. J. Davies, A. Palmer-Julson, et al. (Eds.), *Proceedings of the Ocean Drilling Program, Scientific Results,* Vol. **133**, (pp. 291–300). College Station, TX: Ocean Drilling Program, doi:10.2973/odp.proc.sr.133.233.1993.

Buys, J., Spandler, C., Holm, R. J., & Richards, S. W. (2014). Remnants of ancient Australia in Vanuatu: Implications for crustal evolution in island arcs and tectonic development of the southwest Pacific. *Geology, 42*(11), 939–942.

Campbell, M., Rosenbaum, G., Shaanan, U., Fielding, C. R., & Allen, C. (2015). The tectonic significance of lower Permian successions in the Texas Orocline (eastern Australia). *Australian Journal of Earth Sciences, 62*(7), 789–806.

Cawood, P. A., Hawkesworth, C. J., & Dhuime, B. (2012). Detrital zircon record and tectonic setting. *Geology, 40*(10), 875–878.

Cawood, P. A., Leitch, E. C., Merle, R. E., & Nemchin, A. A. (2011). Orogenesis without collision: Stabilizing the Terra Australis accretionary orogen, eastern Australia. *Geological Society of America Bulletin, 123*(11–12), 2240–2255.

Collins, W. J. (2002). Hot orogens, tectonic switching, and creation of continental crust. *Geology, 30*(6), 535–538.

Davis, B. K., & Henderson, R. A. (1999). Syn-orogenic extensional and contractional deformation related to granite emplacement in the northern Tasman Orogenic Zone, Australia. *Tectonophysics, 305*(4), 453–475.

Ewing, M., Hawkins, L. V., & Ludwig, W. J. (1970). Crustal structure of the Coral Sea. *Journal of Geophysical Research, 75*(11), 1953–1962.

Falvey, A. D., & Taylor, W. H. L. (1974). Queensland plateau and Coral Sea Basin: Structural and time-stratigraphic patterns. *Exploration Geophysics, 5*(4), 123–126.

Feary, D. A., Champion, D. C., Bultitude, R. J., & Davies, P. J. (1993). Igneous and metasedimentary basement lithofacies of the Queensland Plateau (sites 824 and 825). In J. A. McKenzie, P. J. Davies, A. Palmer-Julson, et al. (Eds.), *Proceedings of the Ocean Drilling Program Scientific Results* (pp. 535–540). College Station, TX: Ocean Drilling Program, doi:10.2973/odp.proc.sr.133.254.1993.

Fergusson, C. L., & Henderson, R. A. (2015). Early Palaeozoic continental growth in the Tasmanides of northeast Gondwana and its implications for Rodinia assembly and rifting. *Gondwana Research, 28*(3), 933–953.

Fergusson, C. L., Henderson, R. A., & Offler, R. (2017). Chapter 13 – Late Neoproterozoic to early Mesozoic sedimentary rocks of the Tasmanides, eastern Australia. In R. Mazumber (Ed.), *Sediment provenance. Influences on compositional change from source to sink* (pp. 325–369). Amsterdam: Elsevier.

Foster, D. A., & Goscombe, B. D. (2013). Continental growth and recycling in convergent orogens with large turbidite fans on Oceanic Crust. *Geosciences, 3*(3), 354–388.

Frogtech (2005). OZ Seebase™ study 2005. Public domain report to Shell Development Australia by FrOG Tech Pty Ltd. http://www.frogtech.com.au/ozseebase/

Glen, R. A. (2005). The Tasmanides of eastern Australia. In A. P. M. Vaughan, P. Y. Leat, & R. J. Pankhurst (Eds.), *Terrane processes at the margins of Gondwana* (pp. 23–96). Bath, UK: Geological Society of London Special Publication.

Glen, R. A. (2013). Refining accretionary orogen models for the Tasmanides of eastern Australia. *Australian Journal of Earth Sciences, 60*(3), 315–370.

Glen, R. A., Belousova, E., & Griffin, W. L. (2016). Different styles of modern and ancient non-collisional orogens and implications for crustal growth: A Gondwanaland perspective. *Canadian Journal of Earth Sciences, 53*(11), 1372–1415.

Henderson, R. A., Davis, B. K., & Fanning, C. M. (1998). Stratigraphy, age relationships and tectonic setting of rift−phase infill in the Drummond Basin, central Queensland. *Australian Journal of Earth Sciences, 45*(4), 579–595.

Holcombe, R. J., Stephens, C. J., Fielding, C. R., Gust, D., Little, T. A., Sliwa, R., … Ewart, A. (1997). Tectonic evolution of the northern New England Fold Belt: The Permian–Triassic Hunter-Bowen event. In P. M. Ashley & P. G. Flood (Eds.), *Tectonics and metallogenesis of the New England Orogen* (pp. 52–65). Sydney, NSW: Geological Society of Australia Special Publication.

Hoy, D., & Rosenbaum, G. (2017). Episodic behavior of Gondwanide deformation in eastern Australia: Insights from the Gympie Terrane. *Tectonics, 36*(8), 1497–1520.

Jell, P. A. (Ed.). (2013). *Geology of Queensland*. Brisbane, Qld: Geological Survey of Queensland.

Korsch, R. J., Adams, C. J., Black, L. P., Foster, D. A., Fraser, G. L., Murray, C. G., … Griffin, W. L. (2009a). Geochronology and provenance of the late Paleozoic accretionary wedge and Gympie Terrane, New England Orogen, eastern Australia. *Australian Journal of Earth Sciences, 56*(5), 655–685.

Korsch, R. J., Totterdell, J. M., Cathro, D. L., & Nicoll, M. G. (2009b). Early Permian east Australian rift system. *Australian Journal of Earth Sciences, 56*(3), 381–400.

Leitch, E. C. (1988). The Barnard Basin and the Early Permian development of the southern part of the New England Fold Belt. In J. D. Kleeman (Ed.), *New England orogen – tectonics and metallogenesis* (pp. 61–67). Armidale, NSW: University of New England.

Little, T. A., Holcombe, R. J., Gibson, G. M., Offler, R., Gans, P. B., & McWilliams, M. O. (1992). Exhumation of late Paleozoic blueschists in Queensland, Australia, by extension faulting. *Geology, 20*, 231–234.

Ludwig, K. R. (2003). *Isoplot 3.75 a geochronological toolkit for microsoft excel*. Special publication. Berkeley, CA: Berkeley Geochronology Center, 75 p., 3.75 ed.

Mortimer, N., Campbell, J. H., Tulloch, A. J., King, P. R., Stagpoole, V. M., Wood, R. A., … Seton, M. (2017). Zealandia: Earth's hidden continent. *GSA Today, 27*(3), 27–35.

Mortimer, N., Hauff, F., & Calvert, A. T. (2008). Continuation of the New England orogen, Australia, beneath the Queensland Plateau and Lord Howe Rise. *Australian Journal of Earth Sciences, 55*(2), 195–209.

Mutter, J. C. (1977). *The Queensland Plateau*. Canberra, ACT: Bureau of Mineral Resources, Geology and Geophysics, 55 p.

Paton, C., Hellstrom, J., Paul, B., Woodhead, J., & Hergt, J. (2011). Iolite: Freeware for the visualisation and processing of mass spectrometric data. *Journal of Analytical Atomic Spectrometry, 26*(12), 2508–2518.

Pearce, N. J. G., Perkins, W. T., Westgate, J. A., Gorton, M. P., Jackson, S. E., Neal, C. R., & Chenery, S. P. (1997). A compilation of new and published major and trace element data for NIST SRM 610 and NIST SRM 612 Glass Reference Materials. *Geostandards Newsletter, 21*(1), 115–144.

Petrus, J. A., & Kamber, B. S. (2012). VizualAge: A novel approach to Laser Ablation ICP-MS U–Pb Geochronology Data Reduction. *Geostandards and Geoanalytical Research, 36*(3), 247–270.

Pigram, C. J., & Panggabean, H. (1984). Rifting of the northern margin of the Australian continent and the origin of some microcontinents in Eastern Indonesia. *Tectonophysics, 107*, 331–353.

Rosenbaum, G. (2018). The Tasmanides: Phanerozoic tectonic evolution of eastern Australia. *Annual Review of Earth and Planetary Sciences, 46*, in press.

Rosenbaum, G., Li, P., & Rubatto, D. (2012). The contorted New England Orogen (eastern Australia): New evidence from U–Pb geochronology of Early Permian granitoids. *Tectonics, 31*(1), TC1006. doi:10.1029/2011TC002960

Shaanan, U., & Rosenbaum, G. (2018). Detrital zircons as palaeodrainage indicators: Insights into southeastern Gondwana from Permian basins in eastern Australia. *Basin Research*, *30*(S1), 36–47, doi:10.1111/bre.12204.

Shaanan, U., Rosenbaum, G., & Sihombing, F. M. H. (2017). Continuation of the Ross–Delamerian Orogen: Insights from eastern Australian detrital-zircon data. *Australian Journal of Earth Sciences, 65*. https://doi.org/10.1080/08120099.2017.1354916

Shaanan, U., Rosenbaum, G., & Wormald, R. (2015). Provenance of the Early Permian Nambucca block (eastern Australia) and implications for the role of trench retreat in accretionary orogens. *Geological Society of America Bulletin, 127*(7–8), 1052–1063.

Sircombe, K. N. (1999). Tracing provenance through the isotope ages of littoral and sedimentary detrital zircon, eastern Australia. *Sedimentary Geology, 124*(1–4), 47–67.

Sircombe, K. N., & Hazelton, M. L. (2004). Comparison of detrital zircon age distributions by kernel functional estimation. *Sedimentary Geology, 171*(1–4), 91–111.

Sláma, J., Košler, J., Condon, D. J., Crowley, J. L., Gerdes, A., Hanchar, J. M., … Whitehouse, M. J. (2008). Plešovice zircon – A new natural reference material for U–Pb and Hf isotopic microanalysis. *Chemical Geology, 249*(1–2), 1–35.

Tapster, S., Roberts, N. M. W., Petterson, M. G., Saunders, A. D., & Naden, J. (2014). From continent to intra-oceanic arc: Zircon xenocrysts record the crustal evolution of the Solomon island arc. *Geology, 42*, 1087–1090.

Vermeesch, P. (2012). On the visualisation of detrital age distributions. *Chemical Geology, 312-313*, 190–194.

Appendices

Appendix 1. Sample data

J-CORES sample ID	Sample source	Depth of core below sea floor [m CSF-A]	Sample volume (cm^3)		Composite sample	Concordant (total) U–Pb zircon analyses
KCC000000000005209401	U0824C-18R-1 W, 39.0–41.0 cm	411.89–411.91	10	70	QP-824	63 (96)
KCC000000000005209701	U0824C-18R-1 W, 100.0–102.0 cm	412.50–412.52	10			
KCC000000000005209801	U0824C-18R-1 W, 110.0–112.0 cm	412.60–412.62	10			
KCC000000000005209901	U0824C-19R-1 W, 10.0–12.0 cm	421.30–421.32	10			
KCC000000000005210001	U0824C-19R-1 W, 27.0–29.0 cm	421.47–421.49	10			
KCC000000000005210101	U0824C-19R-1 W, 31.0–33.0 cm	421.51–421.53	10			
KCC000000000005210201	U0824C-19R-1 W, 38.0–40.0 cm	421.58–421.60	10			
KCC000000000005211101	U0825B-9R-1 W, 6.0–9.0 cm	447.06–447.09	10	65	QP-825	33 (227)
KCC000000000005211201	U0825B-9R-1 W, 14.0–16.0 cm	447.14–447.16	5			
KCC000000000005211301	U0825B-9R-1 W, 48.0–51.0 cm	447.48–447.51	10			
KCC000000000005211401	U0825B-9R-1 W, 74.0–76.0 cm	447.74–447.76	5			
KCC000000000005211501	U0825B-10R-1 W, 16.0–20.0 cm	456.86–456.90	5			
KCC000000000005211601	U0825B-10R-1 W, 84.0–86.0 cm	457.54–457.56	10			
KCC000000000005211701	U0825B-10R-1 W, 90.0–92.0 cm	457.60–457.62	10			
KCC000000000005211801	U0825B-10R-1 W, 98.0–100.0 cm	457.68–457.70	10			
KCC000000000005210301	U0824D-9R-1 W, 1.0–4.0 cm	411.51–411.54	10	Photomicrograph (Figure 3)		

Appendix 2. Analytical procedures

Heavy mineral liberation was conducted using high-voltage pulsed power discharges (SelFrag Lab^{TM} S1.1). Magnetic minerals were removed using a Frantz Magnetic Barrier Laboratory Separator (model LB-1) and heavy mineral separates were obtained using di-iodomethane (Methylene Iodide) heavy liquid. Separates were handpicked using a binocular microscope and mounted in a 25 mm diameter mould with Struers Epofix resin. Polarised light and cathodoluminescence-like images of the polished mount were obtained using a Zeiss Axio Imager 2 microscope and Zeiss Sigma SEM (VPSE-G3 detector), respectively. Isotopic compositions were obtained using an ESI New Wave 193 μm laser system with a Trueline ablation cell connected to an Agilent 8800 ICP-MS. Data acquisition involved 25 s of background measurement followed by 30 s of sample ablation using a laser beam diameter of 30 μm. Laboratory procedure involved alternating between approximately 10 zircon grains of unknown ages and 4 reference material analyses. Reference materials include: (1) NIST 610 glass (Pearce *et al.,* 1997) was used as a reference material for trace element determination. (2) Temora 2 (ID-TIMS $^{206}Pb/^{238}U$ age = 416.78 $\pm$ 0.33 Ma, Black *et al.,* 2004) was used as primary reference material. (3 + 4) R33 (ID-TIMS $^{206}Pb/^{238}U$ age = 419.26 $\pm$ 0.39 Ma, Black *et al.,* 2004) and Plešovice (ID-TIMS $^{206}Pb/^{238}U$ age = 337.13 $\pm$ 0.37 Ma, Sláma *et al.,* 2008) were both used as monitor (secondary) reference materials.

Data reduction (instrumental drift, data normalisation, downhole fractionation correction, and age calculation) was conducted using Iolite v3.5 (Paton *et al.,* 2011) with VizualAge v2016.06 (Petrus & Kamber, 2012). The time-resolved isotopic ratios and compositional data for individual ablations were inspected for evidence of open-system behaviour, the mixing of different growth domains, and the presence of inclusions, and other spurious parts of individual analyses were accordingly trimmed before exporting data. Analyses that displayed concentrations of zircon-incompatible elements P, Ti, and La above the third quartile range for granitoids were excluded (Belousova, Griffin, O'Reilly, & Fisher, 2002). Isoplot v4.15 (Ludwig, 2003), DensityPlotter (Vermeesch, 2012) and Microsoft Excel software were used for age calculations and visualisation.

After the exclusion of analyses that were discordant or had clearly anomalous ages, we report weighted mean $^{206}Pb/^{238}U$ ages for the R33 reference material is 424.9 $\pm$ 2.9 Ma (n = 30/41, MSWD = 1.7, probability = 0.009) and Plešovice reference material (346.5 $\pm$ 1.8 Ma, n = 33/40, MSWD = 1.3, probability = 0.12). Note that all age uncertainties herein are presented as propagated 2 sigma error. Error propagation inflates the age uncertainty of an individual unknown zircon by accounting for any excess uncertainties within the primary zircon standard population (Paton *et al.,* 2011).